Journal of Contaminant Hydrology 103 (2009) 194–205

Contents lists available at ScienceDirect

Journal of Contaminant Hydrology

journal homepage: www.elsevier.com/locate/jconhyd

Incorporating layer- and local-scale heterogeneities in numerical simulation of unsaturated flow and tracer transport

Feng Pan [a,e], Ming Ye [b,c,*], Jianting Zhu [a], Yu-Shu Wu [d], Bill X. Hu [c], Zhongbo Yu [e]

[a] Division of Hydrologic Sciences, Desert Research Institute, Nevada System of Higher Education, Las Vegas, NV 89119, United States
[b] Department of Scientific Computing, Florida State University, Tallahassee, FL 32306, United States
[c] Department of Geologic Sciences, Florida State University, Tallahassee, FL 32306, United States
[d] Department of Petroleum Engineering, Colorado School of Mine, Golden, CO 80401, United States
[e] Department of Geosciences, University of Nevada, Las Vegas, NV 89154, United States

ARTICLE INFO

Article history:
Received 12 February 2008
Received in revised form 23 September 2008
Accepted 24 October 2008
Available online 5 November 2008

Keywords:
Unsaturated flow and tracer transport
Heterogeneity
Layer scale
Local scale
Uncertainty analysis
Travel time

ABSTRACT

This study characterizes layer- and local-scale heterogeneities in hydraulic parameters (i.e., matrix permeability and porosity) and investigates the relative effect of layer- and local-scale heterogeneities on the uncertainty assessment of unsaturated flow and tracer transport in the unsaturated zone of Yucca Mountain, USA. The layer-scale heterogeneity is specific to hydrogeologic layers with layerwise properties, while the local-scale heterogeneity refers to the spatial variation of hydraulic properties within a layer. A Monte Carlo method is used to estimate mean, variance, and 5th, and 95th percentiles for the quantities of interest (e.g., matrix saturation and normalized cumulative mass arrival). Model simulations of unsaturated flow are evaluated by comparing the simulated and observed matrix saturations. Local-scale heterogeneity is examined by comparing the results of this study with those of the previous study that only considers layer-scale heterogeneity. We find that local-scale heterogeneity significantly increases predictive uncertainty in the percolation fluxes and tracer plumes, whereas the mean predictions are only slightly affected by the local-scale heterogeneity. The mean travel time of the conservative and reactive tracers to the water table in the early stage increases significantly due to the local-scale heterogeneity, while the influence of local-scale heterogeneity on travel time gradually decreases over time. Layer-scale heterogeneity is more important than local-scale heterogeneity for simulating overall tracer travel time, suggesting that it would be more cost-effective to reduce the layer-scale parameter uncertainty in order to reduce predictive uncertainty in tracer transport.

1. Introduction

Hydrogeologic environments consist of natural soils and rocks that exhibit multi-scale spatial variability, or heterogeneity, in hydraulic and transport parameters from core samples to layer structures and lithofacies. Although the parameters are intrinsically deterministic (i.e., they exist and are potentially measurable at all scales), knowledge of these parameters usually is limited, especially at field scales. Parameter uncertainty thus arises and renders the predictions of contaminant transport uncertain. Quantification of parameter uncertainty and its propagation in hydrogeological models has been studied for decades using stochastic methods, as reviewed in several books (e.g., Gelhar, 1989; Dagan, 1989; Dagan and Neuman, 1997; Zhang, 2002; Rubin, 2003). Quantifying uncertainty at the field scale is of particular importance because decisions are often based on the field-scale predictions. However, field-scale models for representing complex hydrogeologic environments are complicated, making it difficult to evaluate the propagation of parameter uncertainty through the complicated models.

* Corresponding author. Department of Scientific Computing, Florida State University, Tallahassee, FL 32306, United States.
E-mail address: mye@fsu.edu (M. Ye).

0169-7722/$ – see front matter © 2008 Elsevier B.V. All rights reserved.
doi:10.1016/j.jconhyd.2008.10.012

In field-scale modeling, it is common practice to separate a large field domain into hydrogeologic layers (or lithofacies and hydrofacies) based on available data such as site geology, hydrogeology, and geophysics. Hydraulic and transport parameters of each layer often are treated as homogeneous variables and are calibrated to match the field observations of state variables. Layer-scale heterogeneity, especially after layerwise parameters are calibrated, is important in simulating the overall flow and transport trend and pattern. While local-scale heterogeneity within the layers is important in predicting flow path, velocity, and travel time of contaminants, it is often neglected in modeling practices. This study aims to characterize both layer- and local-scale heterogeneities and evaluate their relative effect on the predictive uncertainty in unsaturated flow and contaminant transport.

Our study site is the unsaturated zone (UZ) of Yucca Mountain (YM), which has been recommended by the U.S. Department of Energy (USDOE) as the nation's first permanent geologic repository for spent nuclear fuel and high-level radioactive waste. Since the UZ will host the potential repository and act as an important natural barrier in delaying potential arrival of radionuclides at the water table, it is important to understand how much and how fast water and radionuclides travel through the UZ to the groundwater. The UZ consists of various complex hydrogeologic units, and spatial variability of hydraulic properties in each unit can be viewed as deterministic and/or random processes of multiple scales. Yet, only limited data are available to characterize multi-scale heterogeneities, which results in uncertainty in model parameters and, subsequently, model predictions.

Heterogeneities in the hydraulic properties at the UZ have been investigated by many researchers. Based on the degree of welding, rock properties, and hydraulic properties, the UZ is separated into 5 major geologic units and 33 hydrogeologic layers (Flint, 1998, 2003; BSC, 2003b; Flint et al., 2006). Zhou et al. (2003) categorized the heterogeneity for site, layer, and local scales. Typically, in studies of YM, *site scale* refers to the UZ model domain of numerical modeling studies; *layer scale* refers to the hydrogeologic layers with layerwise average properties; and *local scale* refers to the spatial variation in hydraulic properties within a layer. In the last decade, layer-scale heterogeneity has been characterized and incorporated into the three-dimensional (3-D) site-scale numerical model (e.g., Wu et al., 1999, 2004; BSC, 2004a; Wu et al., 2007). Parameter uncertainty and sensitivity analysis for tracer or radionuclide transport in the YM UZ has been conducted mainly at the layer scale (Nichols and Freshley, 1993; Illman and Hughson, 2005; Zhang et al., 2006; Ye et al., 2007). Local-scale heterogeneity in the model parameters within a layer is also important since it affects the flow path, velocity, and travel time of tracers or radionuclides (Bodvarsson et al., 2001; Haukwa et al., 2003; Zhou et al., 2003; Viswanathan et al., 2003; Illman and Hughson, 2005; Zhang et al., 2006). This study incorporates the layer- and local-scale heterogeneities and conducts a Monte Carlo simulation to investigate their relative importance to the propagation of parameter uncertainty. Based on a-priori knowledge of the UZ described in the Appendix A, the model parameters of particular importance in our local-scale heterogeneity characterizations include matrix permeability and porosity. Since the uncertainty of these two parameters has been characterized at the layer scale in Ye et al. (2007), selecting them for the uncertainty analysis enables us to distinguish between the effects of local-scale and layer-scale heterogeneities on predictive uncertainty of unsaturated flow and tracer transport.

This study is focused on examining the relative effect of layer- and local-scale heterogeneities on predictive uncertainty, but not on jointly assessing the predictive uncertainty due to heterogeneities of the two scales. However, this study can be extended for a joint assessment of multi-scale heterogeneity using, for example, the Random Domain Decomposition (RDD) approach (Winter and Tartakovsky, 2000, 2002; Winter et al., 2002, 2003; Guadagnini et al., 2004; Xiu and Tartakovsky, 2004; Winter et al., 2006). The RDD also separates a field-scale geologic system into a number of geologic units (e.g., hydrogeologic layers and lithofacies), but treats boundaries of the geologic units as uncertain (the units being random composites). The key input of the RDD is the probability of boundary locations, used for averaging local-scale uncertainty to incorporate uncertainty of the unit boundaries. While estimating the probability is still in its development stage (Winter et al., 2006), the problem may be resolved using geostatistical methods (e.g., Guadagnini et al., 2004). When the boundary locations are fixed (e.g., Winter et al., 2006), some results of the RDD can also be obtained by conventional stochastic methods as observed in this study. In terms of separating a highly heterogeneous domain into less heterogeneous hydrogeologic layers, this study is conceptually analogous to the RDD. If uncertainty in the layer boundary locations can be statistically quantified for the UZ, which will be very difficult for the complicated geological system with limited characterization data, this study can be extended to incorporate this uncertainty using the RDD.

2. Characterization of parameter heterogeneity

Fig. 1 presents a typical geological profile along a vertical east–west transect of borehole UZ-14 (shown in Fig. 2) at YM, illustrating a conceptual model currently used to analyze UZ flow patterns and explaining the possible effect of faults and perched water on the UZ system. Details of the conceptual and numerical models for simulating the unsaturated flow and tracer transport are given in the Appendix A. Primarily based on the degree of formation welding, the geologic formations have been organized into five major hydrogeologic units (Montazer and Wilson, 1984): Tiva Canyon welded (TCw) unit, Paintbrush nonwelded (PTn) unit, Topopah Spring welded (TSw) unit, Calico Hills nonwelded (CHn) unit, and Crater Flat undifferentiated (CFu) unit. Due to the intensive characterization of the YM UZ that already has been performed, we consider that boundaries of the units have been delineated with a reasonable degree of accuracy. Each major unit is further divided into several subunits referred to as the hydrogeologic layers.

There are two types of available data for matrix permeability and porosity: core measurements at the local scale and calibrated values at the layer scale. From 33 boreholes, 5320 rock core samples were collected (Flint, 1998, 2003; BSC, 2003b) yielding 546 measurements of saturated hydraulic conductivity (which can be converted to permeability in our simulations) and 5257 measurements of porosity. Particularly,

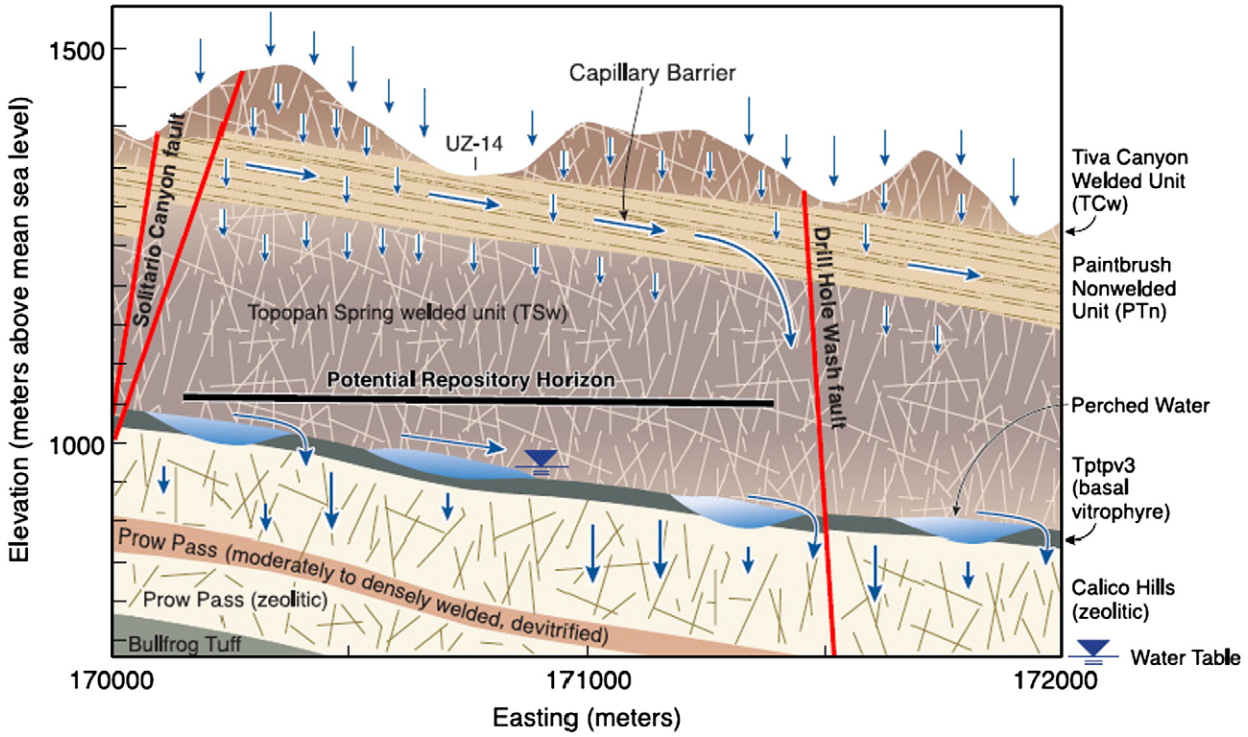

Fig. 1. Schematic illustration of the conceptualized flow processes and effects of capillary barriers, major faults, and perched-water zones within a typical east–west cross section of the UZ flow model domain (modified from BSC, 2004a).

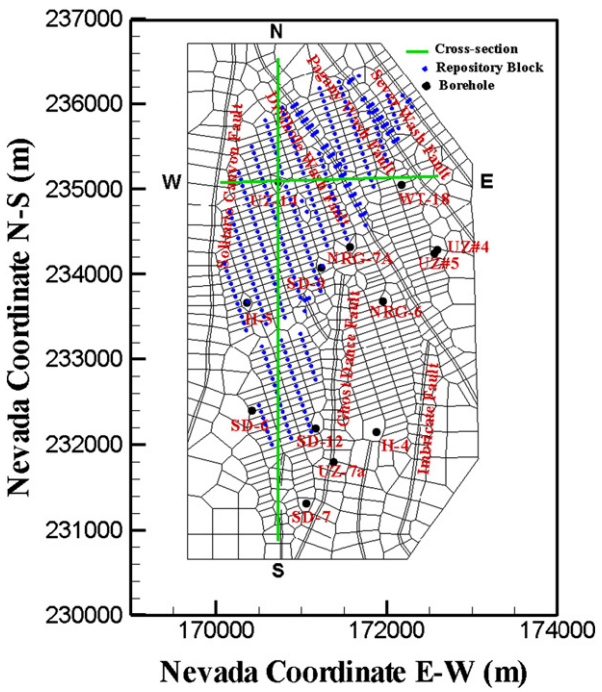

Fig. 2. Plan view of the 3-D UZ numerical model grid shows the model domain, faults, proposed repository layout, and locations of several boreholes (modified from BSC, 2004a). Mean random fields of permeability and porosity along the two cross-sections marked in the figure are shown in Fig. 3.

more porosity measurements are available in shallow boreholes than permeability measurements. Some borehole locations are shown in Fig. 2. The other type of parameter data is the layer-scale values of permeability obtained from calibrating the 3-D model (BSC, 2004a; Wu et al., 2004, 2007). Calibration of the 3-D model is based on calibration of the earlier 1-D model (BSC, 2004b), which resulted in adjustment of the matrix permeability values for the layers BT3, BT2, CHV, and PP3. Since the calibrated permeability values in these layers represent the optimum estimate of layer-scale UZ heterogeneity, the calibrated permeability values for these layers need to be retained in the generated heterogeneous fields.

For each hydrogeologic layer, sequential Gaussian simulation (SGSIM) of GSLIB (Geostatistical Software Library) (Deutsch and Journel, 1998) is used to generate the conditional heterogeneous parameter realizations to characterize local-scale heterogeneity and associated uncertainty. Since the SGSIM does not consider correlation between random variables, the random fields of the matrix permeability and porosity are generated separately. To satisfy the SGSIM requirement for conditional data to be Gaussian (many studies simply assume that the conditioning data are Gaussian), we adopt the transform method of Ye et al. (2007). At each layer, measurements are transformed to be Gaussian by one of the three Johnson transformations (Johnson and Kotz, 1970; Carsel and Parrish, 1988) and four classical re-expressions (Mallants et al., 1996). The random fields incorporating local-scale heterogeneity are first generated with the transformed data and then back-transformed to their real values.

The correlation lengths of the parameters are determined based on variogram analysis. Since the porosity measurements are abundant and widely spread in shallow boreholes, horizontal and vertical correlation lengths of porosity in each hydrogeologic layer of the TCw, PTn, and TSw units are estimated by calculating and fitting the sample variograms. While the vertical variogram of porosity in each hydrogeologic layer of the two deep units of CHn and CFu can be calculated, it is not possible to calculate the horizontal variogram in each layer due to the lack of measurements in the two units. However, we note that, for the three shallow units of TCw, PTn, and TSw, the horizontal correlation length in each layer is similar to that of the unit where the layer belongs. Consequently, horizontal correlation lengths for the layers within the CHn unit are assumed constant and assigned the value of the CHn unit, given that the horizontal variogram of the CHn unit can be calculated from measurements. Since only one borehole was drilled in the CFu unit (below the CHn unit), the horizontal correlation lengths for the two layers in this unit are assumed to be the same as those for the CHn unit. Permeability measurements are sufficient only for estimating the vertical correlation lengths for 14 layers, where there appears to be a tendency for permeability and porosity to have similar vertical correlation lengths. The similarity may be attributed to the strong correlation between permeability and porosity shown in Flint (2003) and to the fact that the permeability and porosity measurements were taken from the same boreholes. It is thus assumed that, for layers where plotting variograms is impossible due to lack of data, the permeability and porosity have the same correlation lengths.

To honor the layer-scale permeability values obtained from the 3-D model calibrations, we first calculate for each numerical block the sample mean (over the realizations) of permeability and then average them over each layer. The resulting layer-averaged values are close to the calibrated values for most model layers, except for layers BT3, BT2, CHV, and PP3, where layer-scale permeability is increased during the model calibration (BSC, 2004a). To ensure that the mean permeability of each realization equals the calibrated value, the layer-averaged permeability is adjusted for the four layers, after which, the generated permeability values are no longer conditioned on the

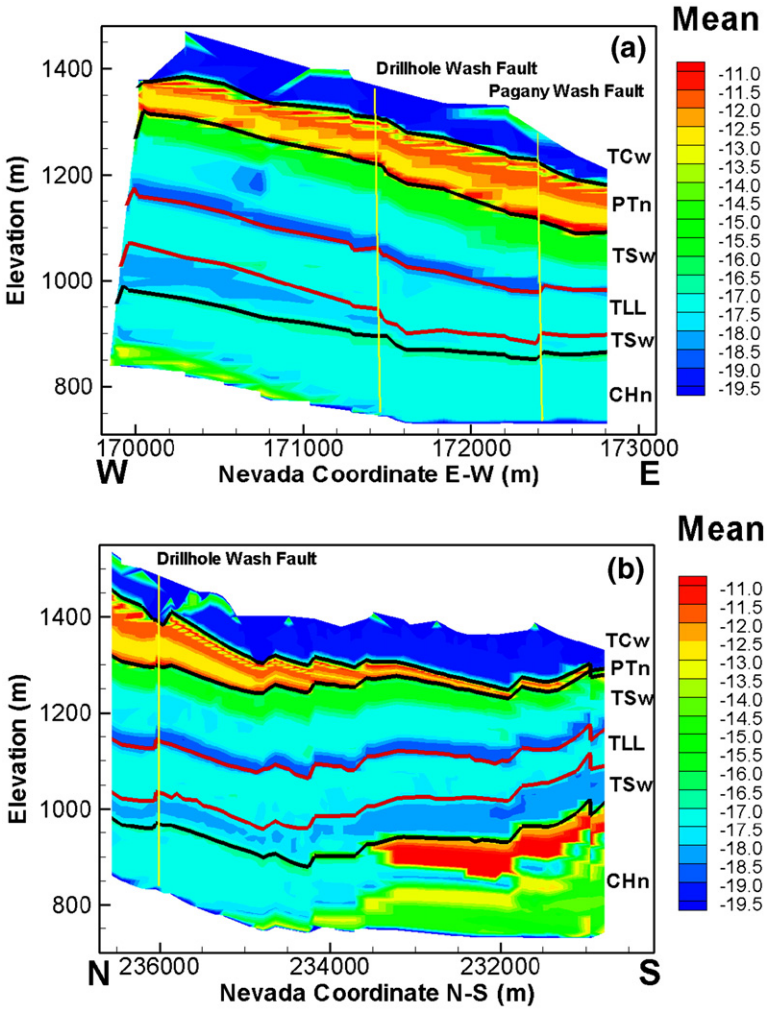

Fig. 3. Mean of generated random log permeability at east–west (a) and north–south (b) cross section through borehole UZ-14 (TCw, PTn, TSw, and CHn are four major units in the UZ of Yucca Mountain; TLL is the proposed repository layer in TSw unit).

local-scale core measurements. As a result, the generated values of permeability and porosity in each layer randomly fluctuate around a mean value that is the same as calibrated layer-scale values or close to them. This procedure omits uncertainty of the calibrated layer-scale parameter values. The ideal way is to compare the probability distribution functions (PDFs) of the layer- and local-scale parameter values. However, estimating the PDFs of the layer-scale variables will require additional field investigation and recalibrating the UZ models, which is beyond the scope of this study.

Fig. 3 plots the sample mean of the 200 realizations of log-permeability at the east–west and north–south cross-sections through borehole UZ-14 located in the proposed repository area (the two cross-sections are marked in Fig. 2). Layer-scale heterogeneity is apparent, since the mean log-permeability is significantly different in the various layers. At the bottom layers, Fig. 3b shows that the mean log-permeability in the northern part of the domain is significantly smaller than that in the south, reflecting the fact that the CHn-unit zeolitic tuffs (with low permeability) are located in the north, while the vitric tuffs (with high permeability) are located in the south. Fig. 3 also illustrates the local-scale heterogeneity within each layer. Sample variance (figures not shown) of the log-permeability over the 200 realizations varies significantly, from 0.5 to 8.0 in different layers, depending on the density of measurements in each layer. In general, the variance is smaller for thinner layers with more measurements. Porosity spatial variability is similar to that of log permeability but with a smaller magnitude of variation.

3. Uncertainty assessments

Monte Carlo simulations are conducted to investigate the propagation of uncertainty in matrix permeability and porosity into the uncertainty in unsaturated flow and tracer transport. The mean, variance, and 5th, 50th, and 95th percentiles of the simulated state variables (e.g., saturation, percolation fluxes, and concentration) are evaluated from 200 realizations. In addition to the variance, the 5th and 95th percentiles (also known as uncertainty bounds) are used to quantify predictive uncertainty. The deterministic simulation results of BSC (2004a) are treated in this study as a baseline case for the stochastic simulations. Note that only layer-scale heterogeneity was considered in the deterministic simulation. Convergence of the Monte Carlo simulations is investigated in a similar manner to Ballio and Guadagnini (2004) and Ye et al. (2004a). Results indicate that the statistics reach stabilization after 150 realizations, and therefore, 200 realizations are regarded sufficient for meaningful statistics for the uncertainty assessments.

3.1. Uncertainty assessment of unsaturated flow

3.1.1. Comparisons of simulated and measured saturation and water potential

Simulated matrix liquid saturation and water potential are verified by comparing their statistics with field observations. Fig. 4 compares the observed and simulated matrix water saturation along borehole SD-12. The simulated mean saturation (as well as the 50th percentile) is close to the corresponding result for the deterministic case (Wu et al., 2004; BSC, 2004a), indicating that layer-scale heterogeneity in model parameters dominates local-scale heterogeneity in simulating the mean behavior of the unsaturated flow. The mean matrix liquid saturation is in reasonable agreement with the observed profiles, especially the matched variation patterns. The 5th and 95th percentiles of simulated results bracket a large portion of the observations, indicating that observed state variability could be explained partially by parameter uncertainty in the

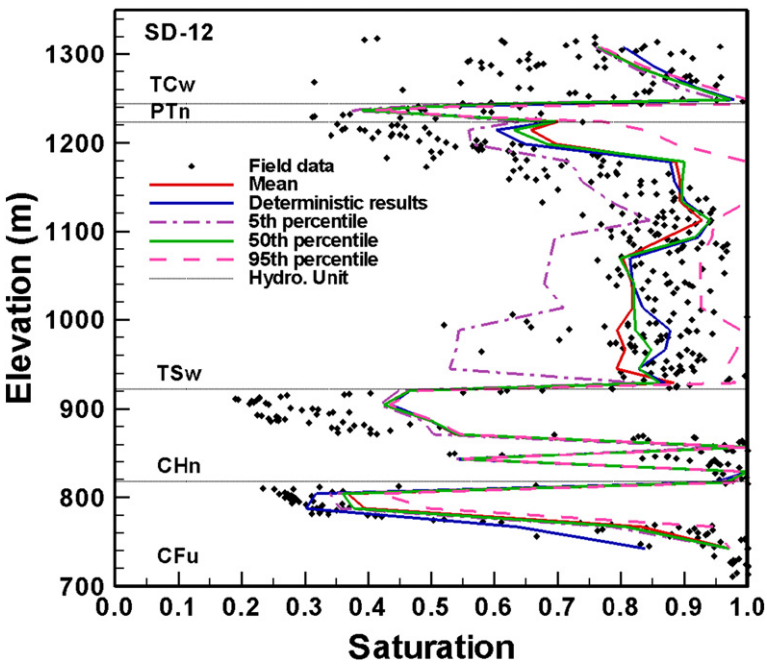

Fig. 4. Comparison of observed and 3-D model simulated matrix liquid saturation for borehole SD-12.

matrix permeability and porosity. Unbracketed measurements may be attributed to uncertainty not considered in this study, such as uncertainty in other model parameters, measurement error, conceptual model incompleteness, and different scales between the model inputs and the field and laboratory parameter measurements. The simulated and observed matrix liquid saturation along other boreholes is also compared, and the comparison results are similar to those shown in Fig. 4. The comparison of simulated and observed water potential along borehole shows similar features as the liquid saturation (figure not shown).

3.1.2. Flow pattern and uncertainty assessments

The percolation flux through the UZ is a key variable in evaluating the potential repository site because percolation flux and its spatial variations could affect the amount of water flowing into the waste emplacement drifts, potential radionuclide release and migration from the UZ to the groundwater table. Percolation flux is defined as the total vertical liquid mass flux through both fractures and matrices (Wu et al., 2004; BSC, 2004a). For better presentation, it is converted to millimeters per year using a constant water density.

Fig. 5 depicts the mean, variance, and 5th and 95th percentiles of simulated percolation fluxes at the proposed repository horizon, while Fig. 6a and b plots the mean and variance at the water table. The pattern of mean percolation fluxes at the proposed repository layer (Fig. 5a) is similar to the surface infiltration pattern, indicating dominant vertical flow and negligible lateral movement from the land surface to the proposed repository level. At the water table (Fig. 6a), the high percolation flux zone moves eastward, indicating significant lateral flow from the proposed repository level to the water table. This is mainly attributed to the dipping slope (around 5 to 10 degrees) and the presence of the CHn unit between the proposed repository and the water table (Fig. 3). Variance in percolation fluxes at the proposed repository level (Fig. 5b) is larger in the western part of the model domain associated with the high infiltration rate. In comparison to Figs. 5b, 6b shows that a large variance at the water table also occurs at the western side of the domain but covers a wider area that extends southward. This may be due to the larger spatial variation of matrix permeability at the bottom than at the top of the simulation domain (Fig. 3) and the accumulated effects of parameter uncertainty propagation downward to the water table. In Fig. 5c and d, the 5th and 95th percentiles of percolation fluxes are significantly different, indicating large uncertainty in the percolation fluxes caused by the uncertainty in matrix permeability.

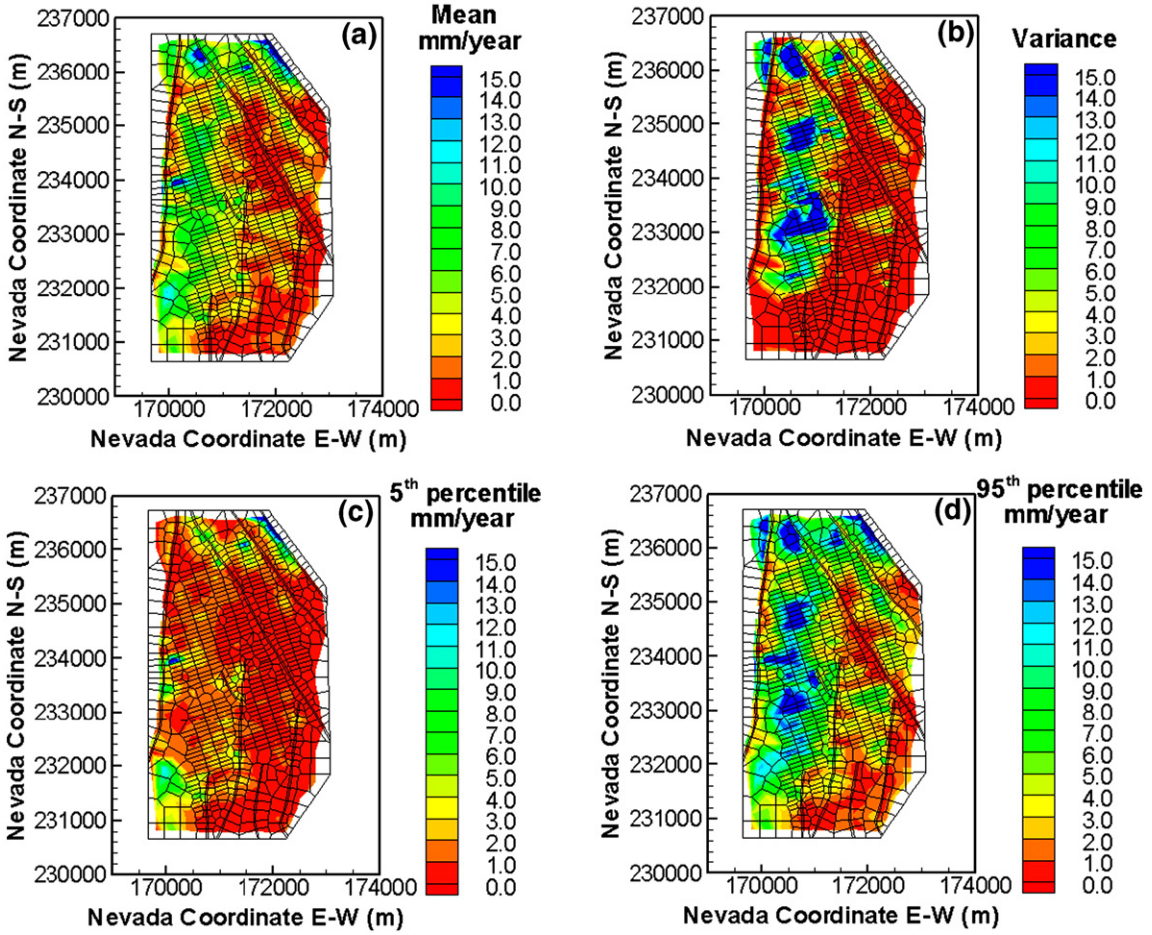

Fig. 5. (a) Mean, (b) variance, (c) 5th percentile, and (d) 95th percentile of simulated percolation fluxes at the proposed repository horizon.

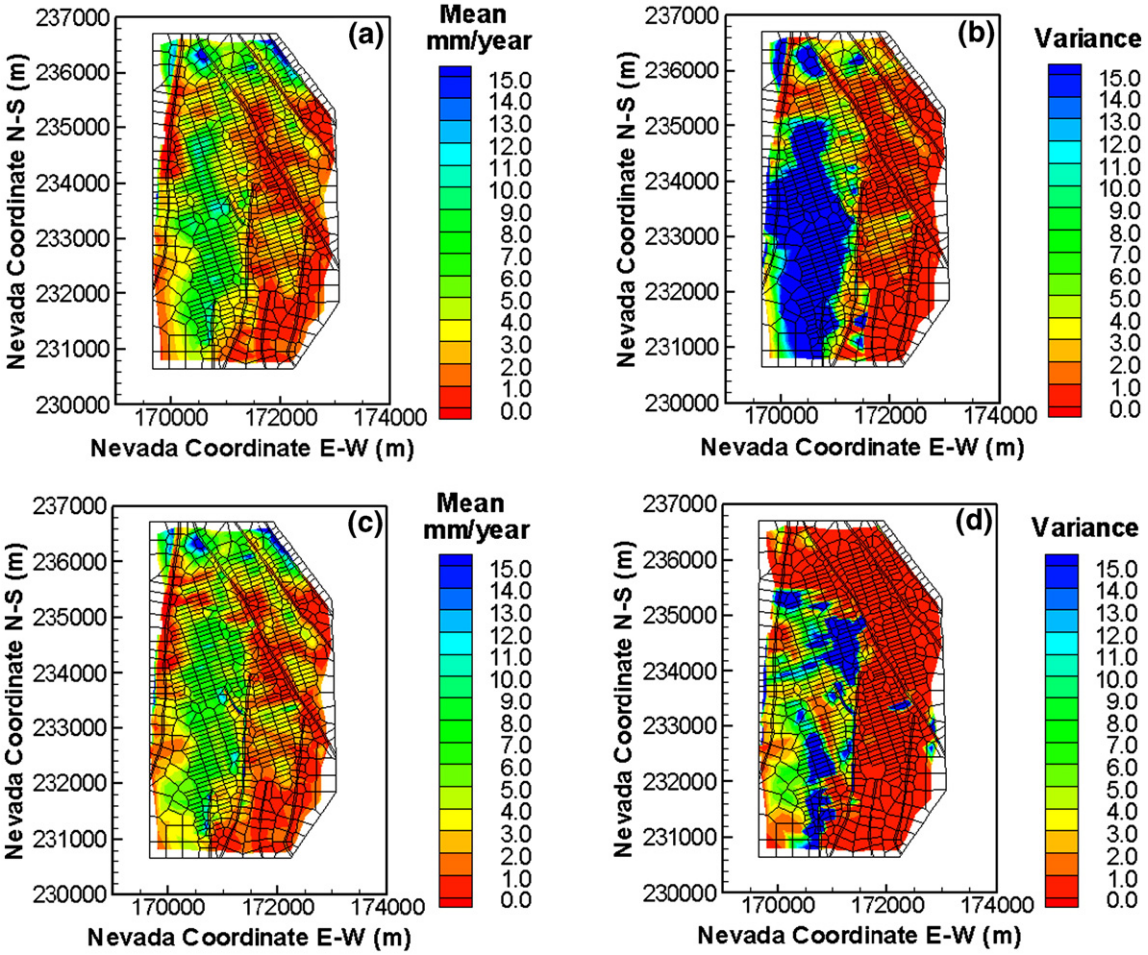

Fig. 6. Mean and variance of simulated percolation fluxes at the water table for the heterogeneous case (a,b) and homogeneous case (c,d).

3.1.3. Comparisons of flow uncertainty assessment

In Ye et al. (2007), the uncertainty of unsaturated flow caused by parameter uncertainty was assessed only at the layer scale. Multiple correlated realizations of matrix permeability and porosity were generated using the Latin Hypercube Sampling (LHS) method for each layer where the parameters were treated as homogeneous. This is referred to as the *homogeneous case*, as opposed to the *heterogeneous case* in this study, where randomly heterogeneous parameter fields are generated for each layer based on the procedure described in Section 2. Fig. 6 plots the mean and variance of the percolation fluxes at the water table for the heterogeneous (Fig. 6a and b) and homogeneous (Fig. 6c and d) cases. While the mean predictions have a similar pattern and magnitude, the variance in the heterogeneous case (Fig. 6b) is significantly larger than that in the homogeneous case (Fig. 6d), especially under the footprint of the proposed repository area shown in Fig. 2. This indicates that the local-scale heterogeneity of matrix permeability results in larger predictive uncertainty in the percolation fluxes because the local-scale heterogeneity creates more complicated flow paths.

3.2. Uncertainty assessment of tracer transport

The uncertainty in tracer transport is evaluated for two representative tracers: conservative (^{99}Tc) and reactive (^{237}Np). Sorption coefficient of ^{237}Np is treated as a random variable, and multiple realizations are generated in the same manner of Ye et al. (2007). Although other transport and geochemical parameters may be also important for the uncertainty assessment, this study treats them deterministically and uses the parameter values of BSC (2004a).

3.2.1. Uncertainty assessment of spatial distribution in tracer plumes

Spatial distribution of the normalized cumulative mass arrival of the tracers is an important variable in evaluating the potential locations of high-radionuclide concentration and migration. The normalized cumulative mass arrival, as defined in BSC (2004a), is the cumulative mass arriving at each cell of the water table over time, normalized by the total mass of the initially released tracer from the potential repository horizon. Fig. 7a and b depicts the mean and variance of the normalized cumulative mass-arrival contours of the reactive tracer

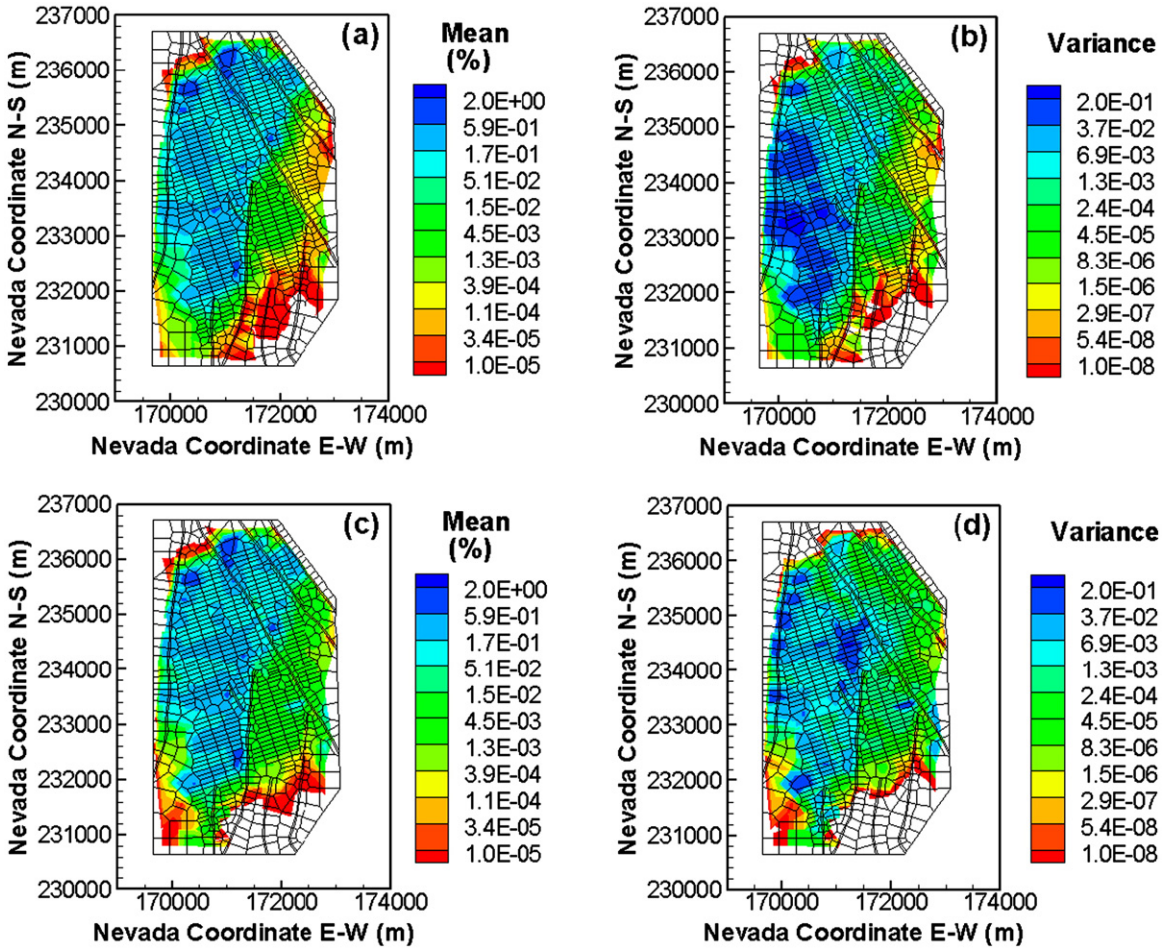

Fig. 7. Contours of mean and variance in normalized cumulative-mass-arrival (%) for the reactive tracer (237Np) at the water table after 1,000,000 years for the heterogeneous case (a,b) and homogeneous case (c,d).

(^{237}Np) at 1,000,000 years (extended standard of the U.S. Environmental Protection Agency). The mean of mass arrival covers virtually the entire area with higher values directly below the footprint of the proposed repository shown in Fig. 2. While the contour spreads widely to the east of the model domain, high values appear restricted to the west of Ghost Dance Fault (Fig. 2, eastern boundary of the repository footprint), indicative of the dominant vertical movement for radionuclides. The variance contour (Fig. 7b) has a similar pattern to the mean contour (Fig. 7a) with higher values of variance below the repository footprint. In addition, the area of higher variance corresponds to the area of high mean, except at the northern end of the Drillhole Wash Fault (Fig. 2). The spatial pattern of variance (Fig. 7b) is correlated with the spatial pattern of percolation flux variance (Fig. 6b), indicating that the larger uncertainty in the percolation flux results in the larger uncertainty in the cumulative mass arrival.

3.2.2. Uncertainty assessment of cumulative mass travel time

Another important factor for assessing performance of the proposed repository is radionuclide travel time from the proposed repository horizon to the water table, since it is a measure of the overall tracer transport. For each of the 200 realizations, the total cumulative mass is calculated by adding the mass in all blocks at the water table. Fig. 8 plots the mean and the 5th and 95th percentiles of the simulated fractional breakthrough curves of cumulative mass arriving at the water table for the two tracers in both heterogeneous and homogeneous cases. For the heterogeneous case, the 5th and 95th percentiles indicate significant uncertainty in travel time. For example, 50% of the total mass of ^{237}Np may take from 31,600 to 295,000 years to arrive at the water table. Owing to the sorption effects of the reactive tracer, the reactive tracer (^{237}Np) travels about two orders of magnitude slower than the conservative tracer (^{99}Tc). For example, the mean travel times of the 50% mass fraction breakthrough is 4760 years for ^{99}Tc, but 109,000 years for ^{237}Np. In comparison to ^{99}Tc, ^{237}Np has greater uncertainty in the fractional mass travel time due to its uncertain sorption coefficient.

3.2.3. Comparison of transport uncertainty assessment

Fig. 7 plots the mean and variance of normalized cumulative mass arrival of ^{237}Np at 1,000,000 years for the heterogeneous (Fig. 7a and b) and homogeneous (Fig. 7c

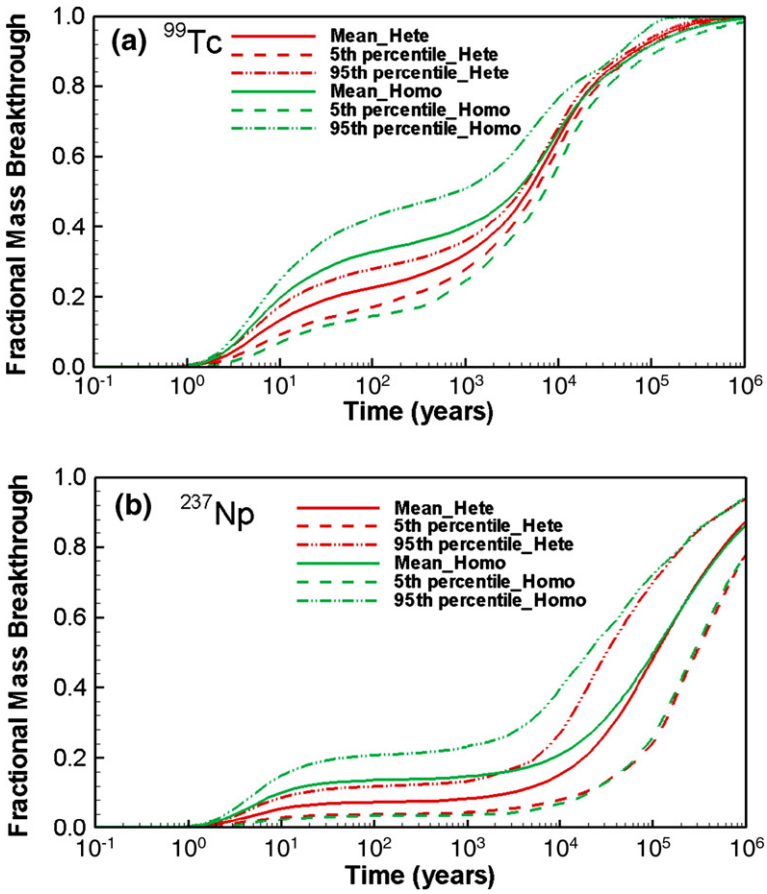

Fig. 8. Simulated breakthrough curves of cumulative mass arriving at the water table for (a) conservative tracer (99Tc) and (b) reactive tracer (237Np) (Hete represents the heterogeneous case and Homo represents the homogeneous case).

and d) cases. While spatial patterns and magnitudes of the mean predictions are similar for the two cases, the variance in the heterogeneous case is much greater than that in the homogeneous case. This comparison suggests that incorporating local-scale heterogeneity of permeability and porosity results in higher uncertainty for radionuclide transport. In other words, it becomes more difficult to estimate potential locations of high-tracer concentration after the local-scale heterogeneity is considered.

Fig. 8 plots the simulated fractional breakthrough curves of cumulative mass arriving at the water table in both heterogeneous and homogeneous cases. The mean travel time for the heterogeneous case increases relative to the homogeneous case for both tracers at the early stage. This observation implies that the simulated flow path becomes more tortuous, and simulated radionuclide transport between matrix and fracture becomes more complicated after the local-scale heterogeneity is considered. With the downward movement of the tracers, since flow paths may develop along the fractures with high permeability, the effect of local-scale heterogeneity of the matrix properties on tracer transport gradually decreases with time. As a result, the travel time in the two cases becomes similar after approximately 20,000 years, with 78% fractional mass breakthrough for ^{99}Tc, and 100,000 years, with 48% fractional mass breakthrough for ^{237}Np. Similar breakthrough behavior was observed in Zhou et al. (2003). Fig. 8 also shows that, for both tracers, the 5th and 95th percentile bound for the travel time prediction is much smaller in the heterogeneous case than in the homogeneous case, indicating the reduced uncertainty in travel time. For example, when 75% of the ^{99}Tc mass flows out of the UZ, the variation in travel time is between 9000 and 23,400 years in the homogeneous case, whereas the variation is between 14,200 and 18,900 years in the heterogeneous case. This difference suggests the importance of layer-scale heterogeneity on controlling the overall pattern of tracer transport measured by travel time of cumulative mass. In the homogeneous case, the layer-scale parameter values vary randomly, rendering significant change in the overall pattern of tracer transport over different realizations. In the heterogeneous case, the layer-scale parameter values are the same or close to the calibrated values over different realizations, despite that the local-scale parameter values vary randomly. Therefore, the overall pattern of tracer transport varies less significantly than in the homogeneous case. This indicates that, if one wants to reduce overall predictive uncertainty in tracer travel time, an effort should be dedicated to reducing uncertainty in layer-scale values by improving the 3-D model calibration of BSC (2004a), recalling that layer-scale values are obtained from inverse modeling.

4. Discussions

At a complicated field site such as the potential YM geological repository, there are two other major sources of uncertainty: uncertainty in conceptual models of the tracer transport and uncertainty in model scenarios capturing all applicable features, events, and processes (FEPs) at the geological repository (BSC, 2003a). Recently, a multi-model averaging method has been advocated to assess the conceptual model uncertainty (Beven and Binley, 1992; Neuman, 2003; Ye et al., 2004b, 2005, 2008a,b; Poeter and Anderson, 2005; Beven, 2006; Refsgaard et al., 2006; Meyer et al., 2007). The study of model scenarios is mainly focused on infiltration (Wu et al., 2002, 2004; Faybishenko, 2007), the major driving force of radionuclide transport to the groundwater. If the conceptual model uncertainty and model scenario uncertainty are considered, the predictive uncertainty will be significantly larger than that caused only by the parameter uncertainty.

Similarly, if additional random parameters are considered, the predictive uncertainty also will increase. As described in the Appendix A, the random parameters are selected mainly based on the sensitivity analysis of Zhang et al. (2006). It would be more rigorous to conduct a comprehensive sensitivity analysis to determine which parameters are influential to predictive uncertainty. In addition, given that the modeling domain is delineated into multiple hydrogeologic layers, and local-scale heterogeneity contributes more to predictive uncertainty than layer-scale heterogeneity, it will be interesting to use sensitivity analysis in determining the layers where local-scale heterogeneity should be considered and the layers where layer-scale heterogeneity would be sufficient. The sensitivity analysis will be useful in optimizing limited computing resources and site characterization for uncertainty reduction.

This research follows the traditional modeling scheme of separating a field-scale modeling domain into less heterogeneous hydrogeologic layers with fixed layer boundaries. Uncertainty in the layer boundaries is not considered in this study. If the uncertainty can be quantified statistically, it can be assessed using the framework of RDD, whereas it will be difficult to obtain reliable quantification of the uncertainty in layer boundaries for the complicated geological systems at the UZ of YM. Although this type of uncertainty is not considered, certain findings of this study (e.g., the relative importance of layer-scale versus local-scale heterogeneities) are similar to those of the RDD method obtained from simulating saturated flow problems.

5. Conclusions

This study leads to the following major conclusions:

(1) Layer-scale heterogeneity is more important than local-scale heterogeneity in simulating the trend and pattern of field observations of flow. Therefore, when simulating the unsaturated flow, layer-scale heterogeneity should be honored by using the calibrated values obtained from the 3-D inverse modeling.
(2) While local-scale heterogeneity slightly affects the mean predictions of percolation fluxes and tracer plumes, it significantly increases predictive uncertainty in these quantities, implying that more random and complicated flow paths are created by the local-scale heterogeneity. This is also true for the spatial distribution of the normalized cumulative mass arrival.
(3) Local-scale heterogeneity increases mean travel time for the reactive and conservative tracers in the early stage, but the effect gradually decreases over time.
(4) Layer-scale heterogeneity is also more important than local-scale heterogeneity in simulating the travel time of cumulative mass to the water table. If one wants to reduce overall predictive uncertainty in tracer travel time, an effort should be made to reduce the uncertainty in layer-scale values by improving the 3-D model calibration, recalling that layer-scale values are obtained from inverse modeling.

Acknowledgments

This work was funded by the U.S. Department of Energy (USDOE) Yucca Mountain Project under a contract between the USDOE and Nevada System of Higher Education. The first author is also supported by the Aileen and Sulo Maki Fellowship from the Desert Research Institute (DRI). The second author conducted part of this research when he was employed by DRI.

Appendix A

This appendix briefly describes the conceptual and numerical models currently used to simulate flow and tracer transport for the UZ. For more details of the models, readers are referred to Wu et al. (1999, 2004, 2007), Wu and Pruess (2000), Flint et al. (2001), and BSC (2004a,c).

A-1 Conceptual model of UZ flow and tracer transport

Percolation flux: The infiltration pulses with spatial and temporal variability from precipitation are major sources of percolation fluxes through the highly fractured TCw unit on the top. The PTn unit with high porosity and low fracture intensity has a large capacity to store the groundwater penetrated through TCw as rapid fracture flow and to form more uniform flux at the base of PTn. The capillary barriers exists within the PTn unit at the upper and lower interfaces with TCw and TSw units due to large contrasts in rock properties across the interfaces (Montazer and Wilson, 1984). The perched water affecting flow paths in the UZ can be found on the top of low-permeability zeolites in CHn unit or the densely welded basal vitrophyre of the TSw unit in several boreholes (e.g., UZ-14, SD-7, SD-9, and SD-12 shown in Fig. 2). In addition, faults with high permeability can play an important role in percolation flux of UZ. More descriptions of flow conceptual model are referred to Wu et al. (2007).

Radionuclide Transport: The radionuclide contaminants can transport through the UZ as dissolved molecular species or in colloidal form, involving the physical processes of advection, molecular diffusion, sorption for reactive tracers, and radioactive decay. The mechanical dispersion through the fracture-matrix system is ignored, since sensitivity studies indicated that the mechanical dispersion has insignificant effect on the cumulative breakthrough curves of tracers at the water table (BSC, 2004a). The sorption processes considers three basic rock types (devitrified tuffs, vitric tuffs, and

zeolitic tuffs). The radionuclide transport in the TSw unit mostly occurs in the fractures. The transport occurs in both matrix and fractures with longer contact times between the radionuclide and the media to lead to the increase of sorption and retardation when radionuclide travels to the vitric layers in CHn unit. However, for those zeolitic layers in CHn unit, fast transport dominated by fractures occurs due to the high disparity in permeability between matrix and fractures in those layers. When radionuclide moves through the devitrified layers in CHn unit, the transport has similar behaviors to the vitric layers. More descriptions of the conceptual model of tracer transport are referred to BSC (2004c).

Features, Events, and Processes (FEPs): The FEPs selected for this study are taken from the LA FEP list included in the Total System Performance Assessment (TSPA). More details of the FEPs can be found in BSC (2003a).

Boundary Conditions and Source Term: For the steady-state flow model, the ground surface and the water table are treated as the top and bottom model boundaries, where the pressure and saturation are specified as boundary conditions. The no-flux boundary condition is specified for the lateral boundaries. A present-day net infiltration estimate is applied to the fracture gridblocks within the second grid layer from the top of the domain, as the first layer is treated as a Dirichlet boundary to represent average atmospheric conditions on the land surface. The transient-state transport simulation was conducted for 1,000,000 years. At the start time of simulation, constant concentration source is instantaneously released from the fracture continuum gridblocks (blue points in Fig. 2) representing the repository (BSC, 2004a). The transport model shares the same boundaries as the flow model, with zero concentration at the top and bottom boundaries and no-flux lateral boundary conditions. More descriptions of the boundary conditions are referred to BSC (2004a,c).

A-2 Numerical modeling approach and model description

A 3-D site-scale numerical model has been developed to simulate the flow and transport of three mass components (air, water, and tracer) in the UZ of YM. Since the dual-continuum approach, primarily the dual-permeability concept, is used, a doublet of governing equations of flow and transport are used to simulate fluid flow, chemical transport, and heat transfer processes in the two-phase (air and water) system of fractured rock for fracture and matrix, respectively. The governing equations for either continuum are in the same form as those for a single porous medium. For more details of the governing equations of the unsaturated flow and tracer transport, the readers are referred to Wu and Pruess (2000) and BSC (2004a,c). The integral finite-difference method is used to solve the governing equations numerically. The 3-D numerical model grid representing the UZ system consists of 980 mesh columns of both fracture and matrix continua along a horizon grid layer, and each column includes an average of 45 model layers representing the hydrogeologic layers. Refined mesh is used near the potential repository and natural faults. Fig. 2 shows the plan view of the 3-D numerical grid with the model domain, proposed repository layout, borehole location, and faults. More details of the numerical model can be found at Wu et al. (1999, 2002, 2004, 2007) and BSC (2004a,b,c).

Model input parameters

Because of the dual-continuum approach, two sets of hydraulic and transport properties and other intrinsic properties are needed for the fractured and matrix continua. The basic parameters used for each model layer include (a) fracture properties (frequency, spacing, porosity, permeability, van Genuchten α and n parameters, residual saturation, and fracture-matrix interface area); (b) matrix properties (porosity, permeability, van Genuchten α and n parameters, and residual saturation); (c) transport properties (grain density, diffusion, adsorption, and tortuosity coefficients); and (d) fault properties (porosity, matrix and fracture permeability, and active fracture-matrix interface area). Assessing uncertainty in all the model parameters is beyond the scope of this study.

This study treats matrix permeability, porosity, and adsorption coefficient as random based on a sensitivity analysis of Zhang et al. (2006), which illustrated that flow and transport simulations are not sensitive to fracture properties because fracture flow dominates over the entire model domain. Although Zhang et al. (2006) found that the matrix van Genuchten α is important, this study treats it as a deterministic variable, since its probabilistic distributions cannot be rigorously identified due to limited number of site measurements (only two or three measurements of the matrix van Genuchten α and n are available in each hydrogeologic layer). Other matrix parameters (e.g., residual saturation) are also considered as deterministic in this study because of their small spatial variability.

References

Ballio, F., Guadagnini, A., 2004. Convergence assessment of numerical Monte Carlo simulations in groundwater hydrology. Water Resour. Res. 40 (5), W04603. doi:10.1029/2003WR002876.

Beven, K., 2006. A manifesto for the equifinality thesis. J. Hydrol. 320, 18–36.

Beven, K.J., Binley, A.M., 1992. The future of distributed models: model calibration and uncertainty prediction. Hydrol. Process. 6, 279–298.

BSC (BECHTEL SAIC Company), 2003a. Total system performance assessment—license application methods and approach. TDR-WIS-PA-000006 REV 00 ICN 01. Bechtel SAIC Company, Las Vegas, Nevada, USA. Electronic version of the report is available at http://www.ocrwm.doe.gov/documents/osti/34865_osti/index.htm.

BSC (BECHTEL SAIC Company), 2003b. Analysis of hydrologic properties data. Report MDL-NBS-HS-000014 REV00. Lawrence Berkeley National Laboratory, Berkeley, CA and CRWMS M&O, Las Vegas, Nevada, USA. Electronic version of the report is available at http://www.ocrwm.doe.gov/documents/amr/32485/index.htm.

BSC (BECHTEL SAIC Company), 2004a. UZ flow models and submodels. Report MDL-NBS-HS-000006 REV02. Lawrence Berkeley National Laboratory, Berkeley, CA and CRWMS M&O, Las Vegas, Nevada, USA. Electronic version of the report is available at http://www.ocrwm.doe.gov/documents/amr/43227osti/index.htm.

BSC (BECHTEL SAIC Company), 2004b. Calibrated properties model. MDL-NBS-HS 000003 REV 02. Lawrence Berkeley National Laboratory, Berkeley, CA and Bechtel SAIC Company, Las Vegas, Nevada, USA. Electronic version of the report is available at http://www.ocrwm.doe.gov/documents/amr/41503/index.htm.

BSC (BECHTEL SAIC Company), 2004c. Radionuclide transport models under ambient conditions. Report MDL-NBS-HS-000008 REV02. Lawrence Berkeley National Laboratory, Berkeley, CA and CRWMS M&O, Las Vegas, Nevada, USA. Electronic version of the report is available at http://www.ocrwm.doe.gov/documents/amr/43226/index.htm.

Bodvarsson, G.S., Liu, H.H., Ahlers, R., et al., 2001. Parameterization and upscaling in modeling flow and transport at Yucca Mountain. Conceptual Models of Flow and Transport in the Fractured Vadose Zone, National Research Council. National Academy Press, Washington, DC, USA.

Carsel, R.F., Parrish, R.S., 1988. Developing joint probability distributions of soil water retention characteristics. Water Resour. Res. 24 (5), 755–769.

Dagan, G., 1989. Flow and Transport in Porous Formations. Springer-Verlag, Berlin, Germany.

Dagan, G., Neuman, S.P., 1997. Subsurface Flow and Transport: A Stochastic Approach. Cambridge University Press, International Hydrology Series Cup, Cambridge, British.
Deutsch, C.V., Journel, A.G., 1998. GSLIB: Geostatistical Software Library and User's Guide, 2nd edition. Oxford University Press, New York, USA.
Faybishenko, B., 2007. Climatic forecasting of net infiltration at Yucca Mountain using analogue meteorological data. Vadose Zone J. 6 (1), 77–92.
Flint, L.E., 1998. Characterization of hydrogeologic units using matrix properties, Yucca Mountain, Nevada. Water Resour. Invest. Rep., vol. 97–4243. US Geological Survey, Denver, Colorado, USA. Electronic version of the report is available at http://pubs.usgs.gov/wri/wri97-4243/#pdf.
Flint, L.E., 2003. Physical and hydraulic properties of volcanic rocks from Yucca Mountain, Nevada. Water Resour. Res. 39 (5), 1–13.
Flint, A.L., Flint, L.E., Bodvarsson, G.S., Kwicklis, E.M., Fabryka-Martin, J., 2001. Evolution of the conceptual model of unsaturated zone hydrology at Yucca Mountain, Nevada. J. Hydrol. 247, 1–30.
Flint, L.E., Buesch, D.C., Flint, A.L., 2006. Characterization of unsaturated zone hydrogeologic units using matrix properties and depositional history in a complex volcanic environment. Vadose Zone J. 5, 480–492.
Gelhar, L.W., 1989. Stochastic Subsurface Hydrology. Prentice Hall, Englewood Cliffs, New Jersey, USA.
Guadagnini, L., Guadagnini, A., Tartakovsky, D.M., 2004. Probabilistic reconstruction of geologic facies. J. Hydrol. 294, 57–67.
Haukwa, C.B., Tsang, Y.W., Wu, Y.-S., Bodvarsson, G.S., 2003. Effect of heterogeneity in fracture permeability on the potential for liquid seepage into a heated emplacement drift of the potential repository. J. Contam. Hydrol. 62–63, 509–527.
Illman, W.A., Hughson, D.L., 2005. Stochastic simulations of steady state unsaturated flow in a three-layer, heterogeneous, dual continuum model of fractured rock. J. Hydrol. 307, 17–37.
Johnson, N.L., Kotz, S., 1970. Distributions in Statistics: Continuous Univariate Distributions, vol. 1. Houghton Miffin Company, Boston, Massachusetts, USA.
Mallants, D., Jacques, D., Vanclooster, M., Diels, J., Feyen, J., 1996. A stochastic approach to simulate water flow in a macroporous soil. Geoderma 10, 299–324.
Meyer, P.D., Ye, M., Rockhold, M.L., Neuman, S.P., Cantrell, K.J., 2007. Combined estimation of hydrogeologic conceptual model, parameter, and scenario uncertainty with application to uranium transport at the Hanford Site 300 Area. Report NUREG/CR-6940, PNNL-16396, prepared for U.S. Nuclear Regulatory Commission, Washington, D.C., USA. Electronic version of the report is available at http://www.nrc.gov/reading-rm/doc-collections/nuregs/contract/cr6940/.
Montazer, P., Wilson, W.E., 1984. Conceptual hydrologic model of flow in the unsaturated zone, Yucca Mountain, Nevada. Water Resour. Invest. Rep., vol. 84–4345. US Geological Survey, Lakewood, Colorado, USA.
Neuman, S.P., 2003. Maximum likelihood Bayesian averaging of alternative conceptual-mathematical models. Stoch. Environ. Res. Risk Assess. 17 (5), 291–305. doi:10.1007/s00477-003-0151-7.
Nichols, W.E., Freshley, M.D., 1993. Uncertainty analyses of unsaturated zone travel time at Yucca Mountain. Ground water 31 (2), 293–301.
Poeter, E.P., Anderson, D.A., 2005. Multimodel ranking and inference in ground water modeling. Ground Water 43 (4), 597–605.
Refsgaard, J.C., van der Sluijs, J.P., Brown, J., van der Keur, P., 2006. A framework for dealing with uncertainty due to model structure error. Adv. Water Resour. 29, 1586–1597.
Rubin, Y., 2003. Applied Stochastic Hydrogeology. Oxford University Press, New York, USA.
Viswanathan, H.S., Robinson, B.A., Gable, C.W., Carey, W.C., 2003. A geostatistical modeling study of the effect of heterogeneity on radionuclide transport in the unsaturated zone, Yucca Mountain. J. Contam. Hydrol. 62–63, 319–336.
Winter, C.L., Tartakovsky, D.M., 2000. Mean flow in composite porous media. Geophys. Res. Lett. 27 (12), 1759–1762.
Winter, C.L., Tartakovsky, D.M., 2002. Groundwater flow in heterogeneous composite aquifers. Water Resour. Res. 38 (8), 1148. doi:10.1029/2001WR000450.
Winter, C.L., Tartakovsky, D.M., Guadagnini, A., 2002. Numerical solutions of moment equations for flow in heterogeneous composite aquifers. Water Resour. Res. 38 (5). doi:10.1029/2001WR000222.
Winter, C.L., Tartakovsky, D.M., Guadagnini, A., 2003. Moment differential equations for flow in highly heterogeneous porous media. Surv. Geophys. 24, 81–106.
Winter, C.L., Guadagnini, A., Nychka, D., Tartakovsky, D.M., 2006. Multivariate sensitivity analysis of saturated flow through simulated highly heterogeneous groundwater aquifers. J. Comput. Phys. 217, 166–175.
Wu, Y.S., Pruess, K., 2000. Numerical simulation of non-isothermal multiphase tracer transport in heterogeneous fractured porous media. Adv. Water Resour. 23, 699–723.
Wu, Y.S., Haukwa, C., Bodvarsson, G.S., 1999. A site-scale model for fluid and heat flow in the unsaturated zone of Yucca Mountain, Nevada. J. Contam. Hydrol. 38, 185–215.
Wu, Y.S., Pan, L., Zhang, W., Bodvarsson, G.S., 2002. Characterization of flow and transport processes within the unsaturated zone of Yucca Mountain, Nevada, under current and future climates. J. Contam. Hydrol. 54, 215–247.
Wu, Y.S., Lu, G., Zhang, K., Bodvarsson, G.S., 2004. A mountain-scale model for characterizing unsaturated flow and transport in fractured tuffs of Yucca Mountain. Vadose Zone J. 3, 796–805.
Wu, Y.S., Lu, G., Zhang, K., Pan, L., Bodvarsson, G.S., 2007. Analysis unsaturated flow patterns in fractured rock using an integrated modeling approach. Hydrogeol. J. 15, 553–572.
Xiu, D., Tartakovsky, D.M., 2004. A two-scale nonperturbative approach to uncertainty analysis of diffusion in random composition. Multiscale Model. Simul. 24 (4), 662–674. doi:10.1137/03060268X.
Ye, M., Neuman, S.P., Guadagnini, A., Tartakovsky, D.M., 2004a. Nonlocal and localized analyses of conditional mean transient flow in bounded, randomly heterogeneous porous media. Water Resour. Res. 40, W05104. doi:10.1029/2003WR002099.
Ye, M., Neuman, S.P., Meyer, P.D., 2004b. Maximum likelihood Bayesian averaging of spatial variability models in unsaturated fractured tuff. Water Resour. Res. 40, W05113. doi:10.1029/2003WR002557.
Ye, M., Neuman, S.P., Meyer, P.D., Pohlmann, K.F., 2005. Sensitivity analysis and assessment of prior model probabilities in MLBMA with application to unsaturated fractured tuff. Water Resour. Res. 41, W12429. doi:10.1029/2005WR004260.
Ye, M., Pan, F., Wu, Y.-S., Hu, B.X., Shirley, C., Yu, Z., 2007. Assessment of radionuclide transport uncertainty in the unsaturated zone of Yucca Mountain. Adv. Water Resour. 30, 118–134.
Ye, M., Meyer, P.D., Neuman, S.P., 2008a. On model selection criteria of multimodel analysis. Water Resour. Res. 44, W03428. doi:10.1029/2008WR006803.
Ye, M., Pohlmann, K.F., Chapman, J.B., 2008b. Expert elicitation of recharge model probabilities for the Death Valley regional flow system. J. Hydrol. 354, 102–115. doi:10.1016/j.jhydrol.2008.03.001.
Zhang, D., 2002. Stochastic Methods for Flow in Porous Media: Coping with Uncertainties. Academic Press, San Diego, California, USA.
Zhang, K., Wu, Y.-S., Houseworth, J.E., 2006. Sensitivity analysis of hydrological parameters in modeling flow and transport in the unsaturated zone of Yucca Mountain. Hydrogeol. J. 14, 1599–1619.
Zhou, Q., Liu, H.H., Bodvarsson, G.S., Oldenburg, C.M., 2003. Flow and transport in unsaturated fractured rock: effects of multiscale heterogeneity of hydrogeologic properties. J. Contam. Hydrol. 60, 1–30.